



## Encapsulation of the quercetin with interpolyelectrolyte complex based on pillar[5]arenes

Anastasia Nazarova<sup>a,\*</sup>, Luidmila Yakimova<sup>a,\*</sup>, Olga Mostovaya<sup>a</sup>, Tatiana Kulikova<sup>a</sup>, Olga Mikhailova<sup>a</sup>, Gennady Evtugyn<sup>a</sup>, Irina Ganeeva<sup>b</sup>, Emil Bulatov<sup>b</sup>, Ivan Stoikov<sup>a,c,\*</sup>

<sup>a</sup>A.M. Butlerov Chemistry Institute of Kazan Federal University, 18 Kremlyovskaya Str., 420008 Kazan, Russia

<sup>b</sup>Institute of Fundamental Medicine and Biology of Kazan Federal University, 18 Kremlyovskaya Str., 420008 Kazan, Russia

<sup>c</sup>Federal Center for Toxicological, Radiation and Biological Safety, 2 Nauchny Gorodok Str., Kazan 420075, Russia

### ARTICLE INFO

#### Article history:

Received 30 August 2022

Revised 26 October 2022

Accepted 12 November 2022

Available online 17 November 2022

#### Keywords:

Pillar[5]arene

Interpolyelectrolyte complexes

Encapsulation

Quercetin

Drug release

### ABSTRACT

The using of pH-sensitive delivery systems is a promising strategy to significantly improve the pharmacological properties of water-insoluble drugs. Herein, we propose and develop an approach to synthesis of interpolyelectrolyte complexes based on combination of two water-soluble decasubstituted non-toxic pillar[5]arenes for encapsulation poor-soluble quercetin and its subsequent release depending on the pH. Interpolyelectrolytes were obtained by mixing aqueous solutions one of which contained a polycationic (ammonium) and the other - a polyanionic (carboxylate) components. The shape and size evolution of interpolyelectrolytes were studied by dynamic light scattering and transmission electron microscopy. Spherical aggregates with an average diameter of 10 nm are found. The ability to form complexes and associates with quercetin by polycationic and polyanionic macrocycle, as well as an interpolyelectrolyte complex based on them, was studied by electron UV-vis and fluorescence spectroscopy, dynamic light scattering. Interpolyelectrolyte complex more efficiently binds quercetin ( $pK_a$  5.13) compared with individual macrocycles due to the greater stability of the associates formed by IPEC. The release of quercetin from the interpolyelectrolyte complex was studied in acidic (pH = 4.00), weakly acidic (pH = 5.00–5.50), neutral (pH = 7.44) and weakly alkaline (pH = 8.15) solutions. It was found the full release of the quercetin without oxidation of flavonoid is observed in the neutral solution. This work provides important guidance for the design of successful delivery systems *via* optimizing the structure and composition of nanocapsules.

© 2022 Elsevier B.V. All rights reserved.

## 1. Introduction

Quercetin is one of the flavonoids, complex heterocyclic compound that is prevalent in the plant kingdom and have antioxidant and antitumor activity due to the ability to absorb free radicals [1,2]. Quercetin belongs to the P vitamins and has anti-inflammatory, antitumor, antispasmodic effects, protects the cardiovascular system and inhibits lipid peroxidation [3–5]. In view of this it is widely used in the treatment of various diseases. Quercetin and dihydroquercetin are protectors of the respiratory system including in the fight against COVID-19 [6,7]. These bioregulators are powerful antioxidants, help strengthen vascular walls, improve microcirculation and prevent dangerous thrombo-

sis, as well as help maintain normal bronchial and lung functions. Also they have an immunomodulatory effect and antiviral activity. Bioflavonoids, such as quercetin and dihydroquercetin, increase the activity of immune cells of T-lymphocytes, B-lymphocytes and macrophages; stimulate the production of interferons and antibodies [8,9]. The activity of quercetin against a number of viruses has been shown, for example, herpes virus type 1, influenza A, respiratory syncytial virus, hepatitis C pathogen [10,11]. It is assumed that the antiviral activity of quercetin is due to its ability to bind with viral envelope proteins and its polymerase enzyme, as well as to damage viral DNA.

Despite these advantages, quercetin has limited therapeutic applications caused by its poor water solubility [12]. Moreover, quercetin is easily oxidized by atmospheric oxygen in moderately alkaline solutions at ambient temperature due to its high activity [13,14]. The use of pH-sensitive delivery systems is a promising strategy to significantly improve the pharmacological properties of quercetin. There are a number of works devoted to the

\* Corresponding authors at: Kazan Federal University, A.M. Butlerov Chemistry Institute, 420008 Kremlyovskaya, 18 Kazan, Russia.

E-mail addresses: [anas7tasia@gmail.com](mailto:anas7tasia@gmail.com) (A. Nazarova), [mila.yakimova@mail.ru](mailto:mila.yakimova@mail.ru) (L. Yakimova), [ivan.stoikov@mail.ru](mailto:ivan.stoikov@mail.ru) (I. Stoikov).

encapsulation of drugs to protect against unwanted degradation processes, including through the formation of host–guest complexes [15–20].

One of the approaches that can increase significantly the solubility of a drug in water and reduce its untimely oxidation is the use of interpolyelectrolyte complexes (IPECs). IPECs [21–25] are associates spontaneously formed by electrostatic interactions, consisting of oppositely charged polyelectrolytes (polycations and polyanions). The main driving force in the formation of IPEC [26] in aqueous solution is the release of low molecular weight counterions previously associated with charged groups of macromolecules. The entropy of the system increases in this case. IPECs can be additionally stabilized by both hydrogen bonding and hydrophobic interactions.

Today, two main approaches to the creation of IPECs based on macrocyclic compounds are presented in the literature [21–26]: 1) the use of polymeric interpolyelectrolytes, which are combined with macrocyclic compounds; 2) the use of ionogenic macrocycles and low molecular weight surfactants. Such IPECs work fairly well and have been extensively studied.

In the presented work, it is proposed to use combination of two decasubstituted water-soluble non-toxic pillar[5]arenes with ionogenic groups as macrocycles containing charged groups for IPEC creation [21,27,28]. The ability of water-soluble pillar[5]arenes to form host–guest complexes in living systems is of great scientific interest, as well as the possibility of their wide practical application [29–32]. Water-soluble pillar[5]arenes can participate in complex formation with various guest molecules and self-organize in solutions due to the presence of polar and non-polar entities in one molecule, the cavity enriched with electrons, the ability to easily vary the nature of substituents. Variation of the stoichiometric ratio through electrostatic interactions will allow changing the surface charge, the stability of colloidal systems and the ability to “pack” biomacromolecules. The novelty of the work is use neither low molecular weight, nor polymeric compounds, but macrocyclic polyelectrolyte complexes with a strictly defined structure. Supramolecular polyelectrolyte is built on these supramolecular blocks: dimers or pairs of pillararenes. This opens up the widest possibilities for their application in medicinal chemistry and pharmacology. It should be noted that these blocks (pillar[5]arenes) are non-toxic, and a variety of nanostructured particles can be assembled from them. It is very important that this class of macrocycles belongs to paracyclophanes, which have a through tubular cavity, and they are chiral. All of the stated above advantages of pillar[5]arene's platform open up limitless possibilities for using this type of polyelectrolytes, which was shown with quercetin as an example. In this regard, the aims of this work were the synthesis of IPECs based on water-soluble pillar[5]arenes containing carboxylate and quaternary ammonium groups, as well as the study of their ability to encapsulate quercetin and its subsequent release depending on the pH. The potential antioxidant properties of encapsulated quercetin were evaluated using cyclic voltammetry.

## 2. Materials and methods

All chemicals were purchased from Acros (Fair Lawn, NJ, USA), and most of them were used as received without additional purification. Organic solvents were purified by standard procedures.  $^1\text{H}$  NMR and  $^{13}\text{C}$  NMR spectra were obtained on a Bruker Avance-400 spectrometer (Bruker Corp., Billerica, MA, USA) ( $^{13}\text{C}\{^1\text{H}\}$  100 MHz and  $^1\text{H}$  400 MHz). Chemical shifts were determined against the signals of residual protons of deuterated solvent ( $\text{D}_2\text{O}$ ). The concentrations of the compounds were equal to 3–5 % by the weight in all the records. All the aqueous solutions were prepared with the Millipore-Q deionized water ( $>18.0\text{ M}\Omega\text{ cm}$  at  $25\text{ }^\circ\text{C}$ ).

**4,8,14,18,23,26,28,31,32,35-Decakis-[(*N*-(2',2'-trimethylammoniummethyl)carbamoylmethoxy)pillar[5]arene decaiodide (1)** was prepared by a literature method [28].

**4,8,14,18,23,26,28,31,32,35-Deca(carboxymethoxy)pillar[5]arene tributylammonium salt (2)** was prepared by a literature method [21].

**4,8,14,18,23,26,28,31,32,35-Deca(carboxymethoxy)pillar[5]arene potassium salt (3)** was prepared by a literature method [27].

### 2.1. Dynamic light scattering (DLS)

#### 2.1.1. Particles' size

The Zetasizer Nano ZS instrument (Worcestershire, UK) equipped with the 4 mW He-Ne laser (633 nm) was used for the determination of particle size. Measurements were performed at a detection angle of  $173^\circ$  and the software automatically determined the measurement position within the quartz cuvette. Processing of the results was performed by the DTS program (Dispersion Technology Software 4.20). The solutions were prepared using deionized water with resistivity  $>18.0\text{ M}\Omega\text{ cm}$ . Deionized water was obtained using a Millipore-Q purification system. In the course of the experiment, the concentrations of **1–3** were  $1 \times 10^{-5}$ ,  $1 \times 10^{-4}$  and  $1 \times 10^{-3}\text{ M}$ . To study the aggregation of interpolyelectrolyte complexes, water solutions of compounds **1–3** ( $2 \times 10^{-3}\text{ M}$ ) were mixed in 1:1 macrocycle/macrocycle ratio. Each subsequent concentration was prepared by 10-fold dilution of a more concentrated previous solution of interpolyelectrolyte complex. The particle sizes were measured after 1 h mixing. Measurements were determined after 24 and 178 h three times to evaluate kinetic stability.

#### 2.1.2. Zeta potentials

Zeta ( $\zeta$ ) potentials were measured on a Zetasizer Nano ZS from Malvern Instruments (Worcestershire, UK). Samples were prepared as for the DLS measurements and were transferred with the syringe to the disposable folded capillary cell for measurement. The zeta potentials were measured using the Malvern M3-PALS method and averaged from three measurements.

### 2.2. Transmission electron microscopy (TEM)

TEM measurements were made at the Interdisciplinary Center for Analytical Microscopy of the Kazan Federal University. Analysis of samples was carried out using a Hitachi HT7700 Exalens transmission electron microscope (Tokyo, Japan) with an Oxford Instruments X-Maxn 80 T EDS detector working in STEM mode. Sample of IPEC ( $1 \times 10^{-3}\text{ M}$ ) was prepared similarly to those studied by the DLS method. 10 mL of the suspension was placed on a carbon-coated 3 mm copper grid and dried at room temperature using special holder for microanalysis. After drying, the grid was placed in the transmission electron microscope and analyzed at an accelerating voltage of 80 kV.

### 2.3. UV-Spectroscopy

Absorption spectra were recorded on a Shimadzu UV-3600 spectrometer (Kyoto, Japan). Quartz cuvettes with an optical path length of 10 mm were used. Deionized water was used for preparation of the solutions. Absorption spectra of mixtures were recorded after an 1 h incubation at  $20\text{ }^\circ\text{C}$ . 150  $\mu\text{L}$  ethanol solution of quercetin ( $6 \times 10^{-4}\text{ M}$ ) was added to those of compounds **1** and **3** ( $3 \times 10^{-5}\text{ M}$ ) in water in a 1:10 ratio and diluted to final volume of 3 mL with water.

## 2.4. Fluorescence spectroscopy

Fluorescence spectra were recorded on the Fluorolog 3 luminescent spectrometer (Horiba Jobin Yvon, Longjumeau, France). The excitation wavelength was selected as 280 nm. The emission scan range was 300–430 nm. Excitation and emission slits were 3 nm for pillararene **3** and IPEC, 5 nm for pillararene **1**. Quartz cuvettes with an optical path length of 10 mm were used. The cuvette was placed at the front face position to avoid the inner filter effect. Fluorescence spectra were automatically corrected by the Fluorescence program. Spectra were recorded at 293 K in water in the presence of 5 % of ethanol. The concentration of the pillararene **1** (**3**) was  $3 \times 10^{-5}$  M and  $1 \times 10^{-5}$  M for IPEC. A  $6 \times 10^{-4}$  M solution of quercetin (0.2, 0.4, 0.6, 0.8, 1, 1.2, 1.4, 1.6, 1.8, 2, 3, 4, 5) in ethanol was added to 0.3 mL of a solution of **1** (**3** or IPEC) ( $3 \times 10^{-4}$  M) in water and diluted to final volume of 3 mL with water. The UV spectra of the solutions were then recorded. The stability constant of complex was calculated by Bindfit [33]. Three independent experiments were carried out for each series.

## 2.5. Analysis of cytotoxicity of IPEC (**1** + **3**) by MTT-assay

### 2.5.1. Cell culture

For IPEC (**1** + **3**) human stromal fibroblasts HSF and human breast carcinoma MCF-7 cells were used. All cell lines were cultured in DMEM media with the addition of 10 % fetal calf serum, 1 mM L-glutamine, penicillin (5000 U/ml) and streptomycin (5,000 µg/ml). Cells were cultured at 37 °C in a humid atmosphere containing 5 % CO<sub>2</sub>.

### 2.5.2. Treatment of cells with test compounds

For IPEC (**1** + **3**) stock solutions of the compounds were prepared by dissolving in sterile Dulbecco's phosphate-buffered saline at a concentration of 4 mM. Cells were treated with the compounds at various concentrations. An equal volume of medium was added to untreated cells as a negative control.

### 2.5.3. Compound Cytotoxicity Analysis

Cytotoxicity analysis of the compounds in tumor cell lines was carried out using standard MTT test to assess the metabolic activity of cells. Results were measured on a plate reader Infinite M200 (Tecan).

Cells were seeded in 96-well flat-bottom culture plates at a concentration of  $3 \times 10^3$  cells per well in a complete culture medium and incubated at 37 °C with 5 % CO<sub>2</sub> for 24 h. Next, cells were treated with IPEC (**1** + **3**) at following concentrations: 10 µM, 20 µM, 40 µM, 80 µM, 160 µM, 300 µM, 500 µM. After addition of the compounds, cells were incubated for 48 h at 37 °C in a humid atmosphere containing 5 % CO<sub>2</sub>. After that MTT reagent was added to each well to a final concentration of 0.5 mg/ml. Then the plates were placed in CO<sub>2</sub> incubator for 3 h. Then, 150 µL of dimethyl sulfoxide (DMSO) was added to each well and plate incubated for another 15 min on a shaker. Optical density was measured at  $\lambda = 590$  nm using plate reader Infinite M200 (Tecan). All measurements were carried out in triplicates. Cell viability was calculated as a relative value with optical density values in the control wells considered as 100 %. Data processing was carried out using the GraphPad Prism6 software.

## 2.6. Electrochemical measurements

Electrochemical measurements were performed at ambient temperature using an Autolab PGSTAT 302 N potentiostat–galvanostat (Metrohm Autolab b.v., the Netherlands). The three-electrode working cell was equipped with the Pt wire as the auxiliary electrode and an Ag/AgCl/3 mol/L KCl reference electrode (Metrohm

Autolab). The quercetin determination was performed on glassy carbon electrode (GCE) which geometric area was determined as 1.67 mm<sup>2</sup>.

The electrode was previously polished on Al<sub>2</sub>O<sub>3</sub> powder and rinsed with deionized water. The working electrode was placed into the working cell with 3 µM or 30 µM of free quercetin or IPEC + quercetin in ABS pH 4.00; H<sub>2</sub>O; PBS pH 8.15 or pH 7.44. All the measurements were performed by running a cycle between –0.2 V and 0.8 V at a scan rate 100 mV/s.

## 3. Results and discussion

Polyion functionalized platforms are widely used in biomedicine, catalysis, cosmetics, oil production and other fields [34–47]. A key domain of their application is biotechnology, namely, polyelectrolyte encapsulation and the creation of nanocontainers for targeted delivery, storage, and prolonged release of biologically active compounds [48–50]. In this regard, the search for new supramolecular host molecules and their adaptation for biomedical diagnostics are highly sought in the supramolecular chemistry and in medical diagnostics. A promising macrocyclic platform for creating such self-assembling nanostructures is the macrocycles discovered in 2008 – pillar[5]arenes [51]. The interaction of pillar[5]arenes with drugs is being actively studied. Such complexes can be used to increase the solubility of some drugs, reduce their toxicity to the body, as molecular recognition systems, biosensors, and also as systems for the targeted delivery of drug compounds [31].

### 3.1. Synthesis of IPECs based on water-soluble pillar[5]arenes

We used cationic and anionic pillar[5]arenes **1–3** synthesized earlier [21,28] in our research group to create IPECs with different particle sizes and stability (Fig. 1). The self-assembly study of individual components **1–3** in water by dynamic light scattering (DLS) showed (Table 1) the formation of polydisperse systems in the studied range of concentrations ( $1 \times 10^{-5}$  –  $1 \times 10^{-3}$  M).

The next stage was the creation of interpolyelectrolyte complexes (IPECs) based on the self-assembly of water-soluble oppositely charged pillar[5]arenes. Interpolyelectrolytes were obtained by mixing aqueous solutions one of which contained a polycationic (**1**) and the other – a polyanionic component (**2**, **3**). The aggregation properties of IPECs were studied by the DLS in water in the concentration range  $1 \times 10^{-5}$  –  $1 \times 10^{-3}$  M (Table S1). A bimodal distribution of associates is observed (Table 2), as expected, for the **1** + **2** system. The possible reason is competition the quaternary ammonium fragment of pillararene **1** and the tributylammonium cation for the carboxylate group of macrocycle **2**. In addition to micron aggregates, submicron aggregates are formed (Table 2) that are broken down over time. While for IPEC formed by macrocycles **1** and **3**, the formation of monodisperse nanometer associates was shown (Table 2). The value of the zeta potential (1.98 mV) of the IPEC (**1** + **3**) close to zero, apparently, indicates the compensation of the negative and positive

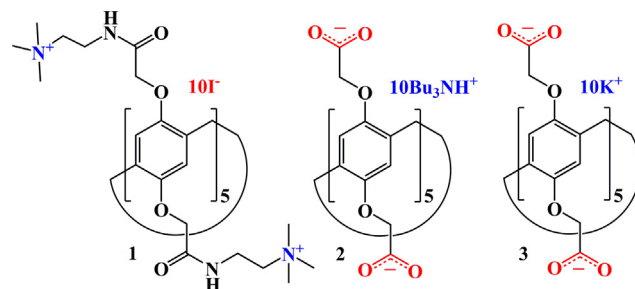


Fig. 1. Structures of pillar[5]arenes as components of the IPECs.

**Table 1**  
Sizes of aggregates (diameter (d) of compounds **1**, **2** and **3**) and the corresponding polydispersity indexes (PDI), (H<sub>2</sub>O, 298 K).

Compound	C, M					
	$1 \times 10^{-5}$		$1 \times 10^{-4}$		$1 \times 10^{-3}$	
	d, nm	PDI	d, nm	PDI	d, nm	PDI
<b>1</b>	466 ± 305	0.50 ± 0.10	255 ± 38	0.44 ± 0.08	199 ± 51	0.47 ± 0.05
<b>2</b>	306 ± 42	0.37 ± 0.11	360 ± 72	0.42 ± 0.16	234 ± 192	0.70 ± 0.25
<b>3</b>	390 ± 121	0.59 ± 0.34	277 ± 68	0.36 ± 0.09	162 ± 32	0.45 ± 0.10

**Table 2**  
Hydrodynamic diameters, polydispersity indexes (PDI) and zeta potential ( $\zeta$ ) of interpolyelectrolyte systems **1 + 2** and **1 + 3** (H<sub>2</sub>O, 298 K).

IPEC	<b>1 + 2</b> , 1:1 ( $1 \times 10^{-5}$ M)			<b>1 + 3</b> , 1:1 ( $1 \times 10^{-3}$ M)		
	d, nm	PDI	$\zeta$ , mV	d, nm	PDI	$\zeta$ , mV
	216 ± 31 (94.6 %)	0.34 ± 0.05	N/A*	9.2 ± 0.2	0.08 ± 0.01	1.98
	3062 ± 293 (5.4 %)					

\* N/A – not applicable.

charges of individual molecules in a 1:1 ratio. Moreover, such value of the zeta potential of the system is probably due to the small size of the resulting particles, which have a smaller diffuse layer.

The stability of the resulting IPEC (**1 + 3**) in the  $1 \times 10^{-3}$  M (Table 3) concentration was also evaluated in saline and Ringer-Locke solution. It was shown that the monomodal distribution of nanoparticles saved both in saline and Ringer-Locke solution, while the zeta potential is almost unchanged (1.72 and 1.91 mV correspondingly). Obviously, the salt effect of solutions (saline and Ringer-Locke) leads to a decrease in the nanoparticles size due to the salting effect.

Nanoaggregates formed by IPEC (**1 + 3**) were studied by transmission electron microscopy. TEM data on particle sizes are in good agreement with the data obtained earlier by the DLS (Fig. 2). Spherical aggregates with an average diameter of 10 nm (Fig. 2) are formed from a **1 + 3** mixture (the ratio of macrocycles is 1:1) after evaporation of the solvent. Thus, nano-sized IPECs were created based on the water-soluble ammonium pillar[5]arene **1** and the potassium salt of the carboxylate pillar[5]arene **3**, which were further investigated for the ability to interact with quercetin.

### 3.2. Analysis of cytotoxicity of IPEC complex by MTT-assay

In recent years, IPECs used as drug delivery systems are of great scientific interest in the chemistry and pharmacology. One of the main requirements for such systems is the absence of any toxicity. In this respect the next step of investigation was to study the cytotoxicity of the synthesized IPEC.

The cytotoxic effect of the IPEC (**1 + 3**) have been studied to human stromal fibroblasts HSF and human breast carcinoma MCF-7 cells in MTT assay. In the studied concentration range IPEC (**1 + 3**) did not lead to a reduction in cell viability below 50 %. Based on these results, it can be concluded that the compounds are not toxic at the studied concentrations (Fig. 3). It is also important to note that metabolic activity of cells was enhanced after treated with IPEC mixture.

**Table 3**  
Hydrodynamic diameters, polydispersity indexes (PDI) and zeta potential ( $\zeta$ ) of interpolyelectrolyte system **1 + 3** (298 K).

IPEC ( <b>1 + 3</b> )	Saline			Ringer-Locke solution		
	d, nm	PDI	$\zeta$ , mV	d, nm	PDI	$\zeta$ , mV
	4.5 ± 0.3	0.15 ± 0.02	1.72	4.3 ± 0.2	0.25 ± 0.01	1.91

### 3.3. Complexing properties of water-soluble pillar[5]arenes and IPECs based on them with respect to quercetin

The ability to form complexes with quercetin by polycationic pillar[5]arene **1** and polyanionic macrocycle **3**, as well as an IPEC based on them, was studied by electron absorption spectroscopy, dynamic light scattering, NMR and fluorescence spectroscopy.

In order to study the complexation of pillar[5]arenes **1** and **3** with quercetin (Q) in the binary system (H<sub>2</sub>O + 5 % EtOH), solution of quercetin (Q) with C =  $3 \times 10^{-5}$  M was added to the solutions of compound **1** or **3** ( $C_{\text{macrocycle}} = 3 \times 10^{-6}$  M). A slight deflection (hyperchromic effect) of the optical density of the mixture ( $A_{\text{complex}}$ ) from the additive spectrum of the components ( $\Sigma A_{\text{mixture}}$ ),  $\Delta A = A_{\text{complex}} - \Sigma A_{\text{mixture}}$  was shown for both systems which indicates the interaction of individual macrocycles with the guest-molecule (Fig. S5).

The association study was also carried out in the binary system (H<sub>2</sub>O + 5 % EtOH) by adding a quercetin solution to the IPEC (**1 + 3**) solution (C =  $3 \times 10^{-5}$  M) (Fig. 4). It was found that the interaction between IPEC (**1 + 3**) and quercetin was accompanied by a bathochromic shift of the quercetin absorption band in the region of 366 nm and a rise in the baseline. This is indicated by the formation of a dispersed system (Fig. 4).

The study of the presented systems was supplemented by the DLS. The ability of IPEC (**1 + 3**) to self-assemble in the presence of quercetin was studied. It was found (Table S2) that the formation of polydisperse systems occurred (PDI =  $0.35 \pm 0.21$ ) in the case of all the studied mixtures (**1 + Q**, **3 + Q**, IPEC + Q).

Complexation between the individual pillar[5]arenes **1**, **3**, IPEC and quercetin was also studied by <sup>1</sup>H and 2D <sup>1</sup>H-<sup>1</sup>H NOESY NMR spectroscopy (Fig. 5, Fig. S6). Unfortunately, the carboxylate derivative of pillar[5]arene **3** has poor solubility at this concentration ( $5 \times 10^{-3}$  M or  $1 \times 10^{-2}$  M) in organic solvents, which were proposed to be used for recording two-dimensional NMR spectra. In this regard, the 2D NOESY NMR spectrum was recorded only for a mixture of ammonium pillar[5]arene **1** with quercetin. Thus,

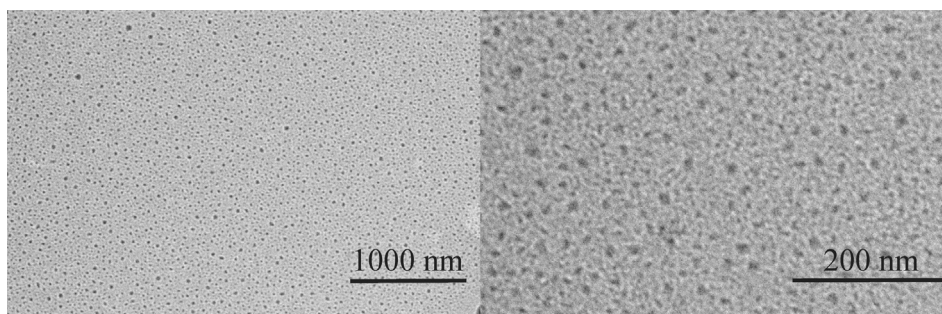


Fig. 2. TEM images of aggregates formed by IPEC (1 + 3),  $1 \times 10^{-3}$  M.

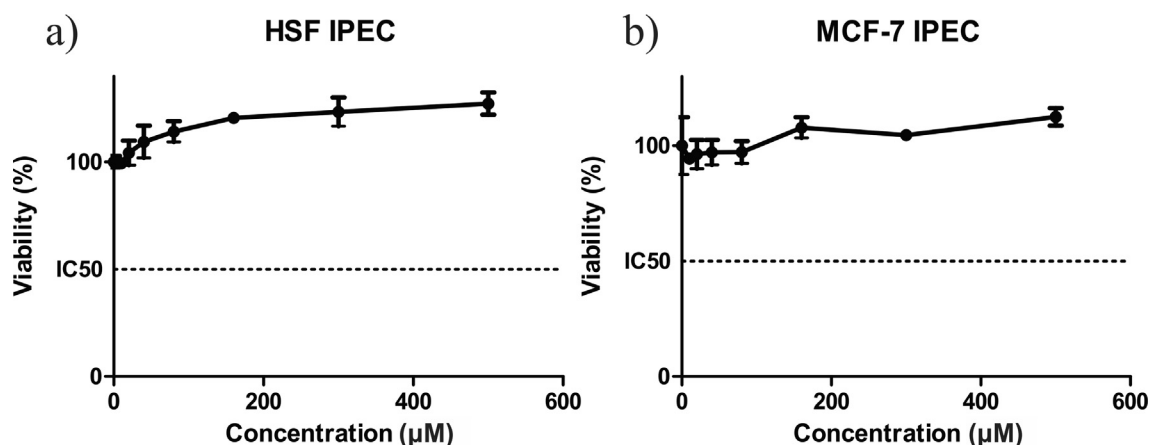


Fig. 3. Cytotoxicity of IPEC (1 + 3) in: a) human stromal fibroblasts (HSF); b) MCF-7 cells.

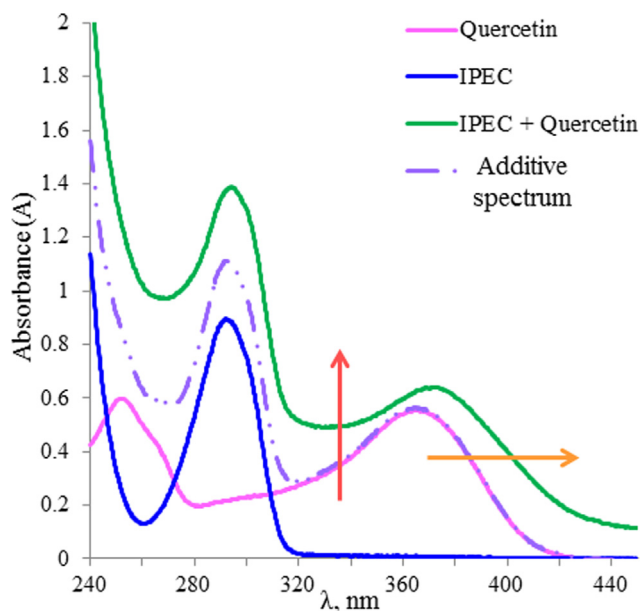


Fig. 4. Electronic absorption spectra for the IPEC (1 + 3) / quercetin in an equimolar ratio ( $C_{\text{IPEC}} = 3 \times 10^{-5}$  M,  $C_{\text{guest}} = 3 \times 10^{-5}$  M).

it was shown (Fig. S6) that in the  $^1\text{H}$  NMR spectrum of the mixture there are practically no changes in the proton signals of pillar[5]arene **1**. Almost all proton signals of quercetin are shifted to the weak field by 0.01–0.02 ppm (Fig. S6). Two-dimensional  $^1\text{H}$ – $^1\text{H}$  NOESY NMR spectrum of a mixture of macrocycle **1** with quercetin in DMSO showed (Fig. 5) the presence of cross peaks between the

methyl protons  $\text{H}^7$  of pillar[5]arene and the protons of the hydroxyl group of quercetin  $\text{H}^b$ . Also there are cross peaks between the  $\text{H}^a$  and  $\text{H}^c$  aromatic protons of quercetin and the  $\text{H}^7$  methyl protons at the quaternary nitrogen atom of pillar[5]arene.

Based on the obtained results for the host/guest system, it can be assumed that quercetin does not enter the macrocyclic cavity and the interaction occurs only with pillararene substituents, as shown in the Fig. 5b.

Today, fluorescence spectroscopy is widely used in studies with biologically active molecules. Fluorescence spectroscopy being a highly sensitive and selective method captures the slightest changes in the environment of the studied particles [52]. It was shown that the fluorescence of pillar[5]arenes **1**, **3** and the IPEC was quenched (Fig. S7) in the presence of quercetin, which indicated the interaction of pillar[5]arenes with quercetin. A fluorometric titration was performed to quantify this interaction. The concentration of macrocycles remained constant for pillar[5]arene **1**/Q (Fig. 6a), pillar[5]arene **3**/Q (Fig. S8), IPEC (1 + 3)/Q (Fig. 6b) systems, while the concentration of quercetin increased from a ratio of 1:0.2 to 1:5 (Fig. 6). Linearization of the obtained titration curves using BindFit [33] made it possible to calculate the association constants of complexes with the composition 1:1 (Fig. S9–S11). The logarithm of the association constant for the system pillar[5]arene **3**/Q was defined as  $\lg K_a(\mathbf{3} + \text{Q}) = 4.14$  (Fig. S9). The logarithms of the association constant were  $\lg K_a(\mathbf{1} + \text{Q}) = 4.36$  (Fig. S10) for **1**/Q and  $\lg K_a(\text{IPEC} + \text{Q}) = 5.13$  (Fig. S11) for the IPEC (1 + 3)/quercetin (Fig. S11). The stoichiometry of the complex was also confirmed by titration data processed using host:guest ratios of 1:2 and 2:1 (Fig. S9–S11). However, in this case the association constant of the complexes was determined with a large error.

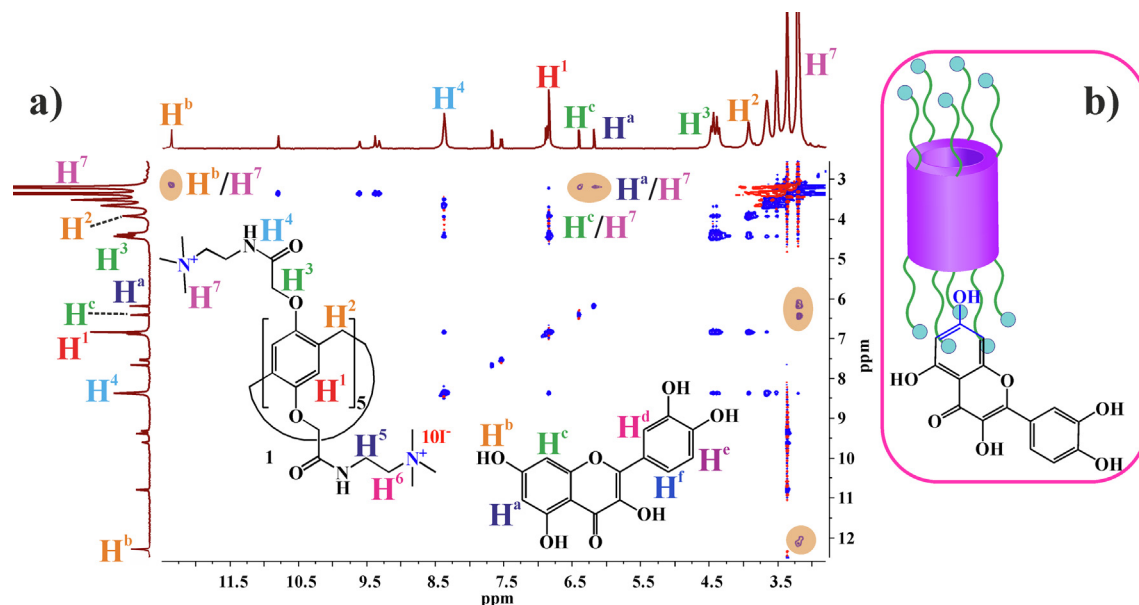


**Fig. 5.** A) 2D  $^1\text{H}$ - $^1\text{H}$  NOESY NMR spectrum of the **1** + quercetin mixture,  $C_{\text{Host}} = C_{\text{Guest}} = 1 \times 10^{-2}$  M (DMSO  $d_6$ , 298 K, 400 MHz); b) schematic representation of complex formation between pillar[5]arene **1** and quercetin.

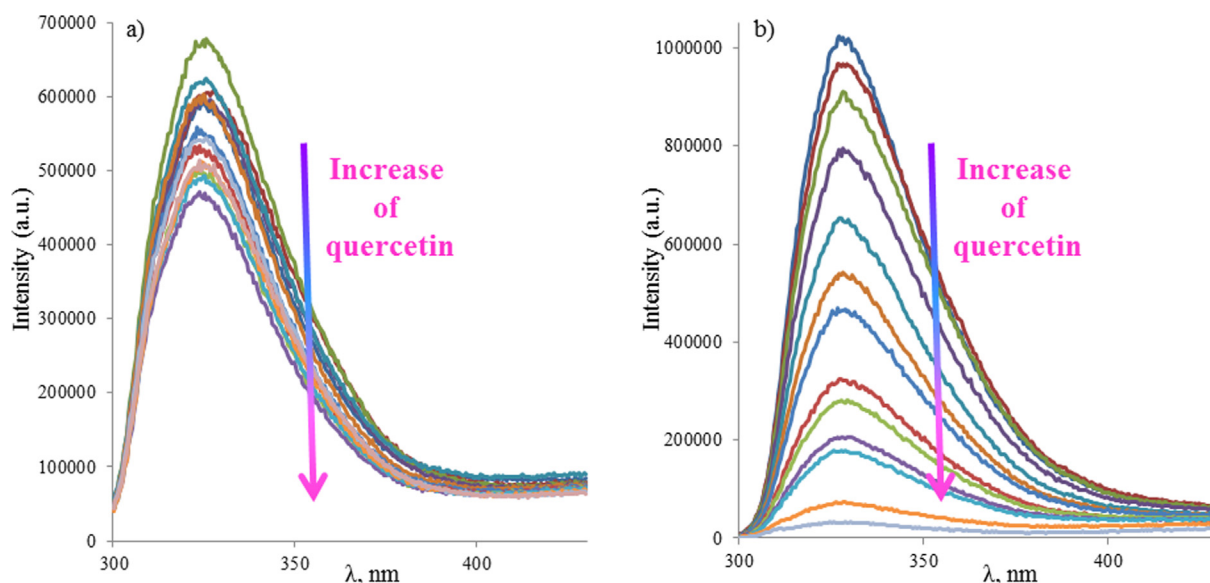


**Fig. 6.** (A) Fluorescence spectra of pillar[5]arene **1** (a) and IPEC (**1** + **3**) (b) with different concentrations of quercetin (from 0.2 to 5-fold excess) in binary system ( $\text{H}_2\text{O}$  + 5 % EtOH).

The difference between the logarithms of the association constant of the initial pillar[5]arenes **1** and **3** compared to the IPEC is apparently due to the formation of stable associates (Table 2) by two oppositely charged macrocycles ( $d = 9.2 \pm 0.2$  nm,  $\text{PDI} = 0.08 \pm 0.01$ ), which leads to higher preorganization of complex and more efficient binding of guest-molecules. Analysis of the literature data [21,26,53,54] and the results obtained allows us to suggest that the structure of the polyelectrolyte complex is similar to micelles and the binding of quercetin occurs due to the hydrophobic effect and  $\pi$ - $\pi$  interaction.

### 3.4. Study of the quercetin release from IPEC at different pH

Complexes of water-soluble pillar[5]arenes with drugs have a prospect of practical application if the binding occurs reversibly.

It means that the drug is bound under certain conditions, and it is released due to the destruction of the complex when the media changes [55,56]. Thus, the next step was to study the possibility of quercetin released from an equimolar complex with an IPEC ( $C = 3 \times 10^{-6}$  M) under the change in the pH solution. For this purpose, solutions of the ternary system (IPEC + Q) were prepared in acetate buffer (pH = 4.00, pH = 5.00 and pH = 5.50), phosphate buffer (pH = 7.44 and pH = 8.15), and in an aqueous solution. The degree of quercetin release from the ternary system was assessed by the change in the absorption intensity of the quercetin band at 366 nm. It is well known that two chromophore centers [57] in the absorption spectrum of flavonoids correspond to two absorption bands (Fig. 7). The first one is in the range of 340–380 nm, which is associated with the absorption of light by “A” part of the quercetin molecule. And the other is in UV region (280–

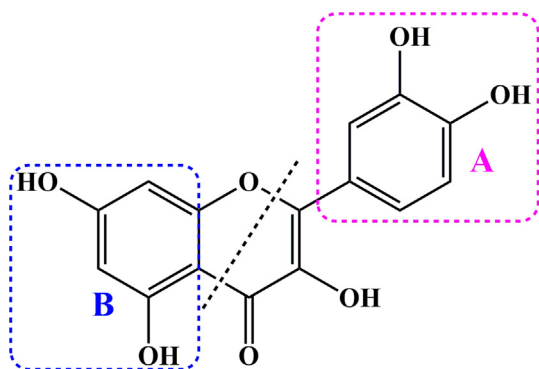


Fig. 7. Structure of quercetin.

340 nm), corresponding to the absorption of light by the “B” ring. The most sensitive band to environmental conditions and chemical interaction is the one corresponding to part “A”. The changes in the spectra within wavelength 340–380 nm were used to interpret the processes of release from IPEC occurring in solutions.

An aliquot of an aqueous-alcoholic solution of the equimolar IPEC + Q complex with a volume of 300  $\mu\text{L}$  ( $C = 3 \times 10^{-5}$  M) was diluted 10 times with a buffer solution (water). The change in the absorption of the resulting solutions was observed over time: immediately after preparation (1 min), after 15 and 30 min, after 60 min, after 120 min, and one day after the preparation of the solution. An aqueous solution was used as a reference solution. Thus, an insignificant rise in the baseline was observed (Fig. 8a) when an aliquot of the ternary system solution was diluted with water.

A slight increase in the absorption intensity of quercetin at 366 nm (Fig. 8b) occurs immediately after mixing in the case of dilution of an aliquot of the ternary system with a phosphate buffer solution with neutral pH = 7.44. It decreases with time, and absorption band shifts to the red region of the spectrum. It is worth noting the rise in the baseline over time, which additionally indicates the release of quercetin in phosphate buffer. Gradual release of quercetin from the ternary system leads to precipitation in view of low solubility of quercetin in aqueous and buffer media, which causes a rise in the baseline in electronic absorption spectra (Fig. 8b). There is an additional decrease in the absorption intensity of quercetin and the absence of a rise in the baseline while main-

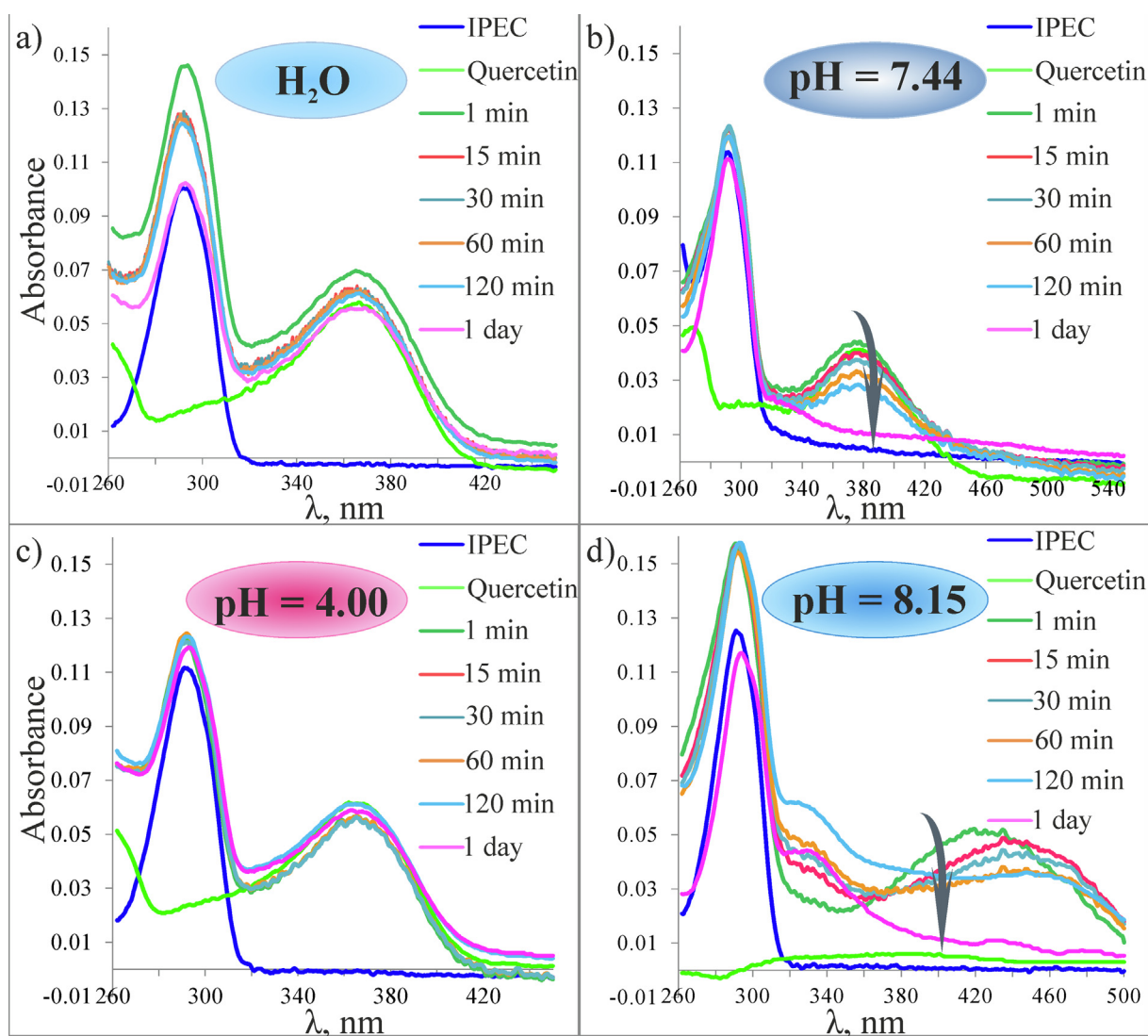
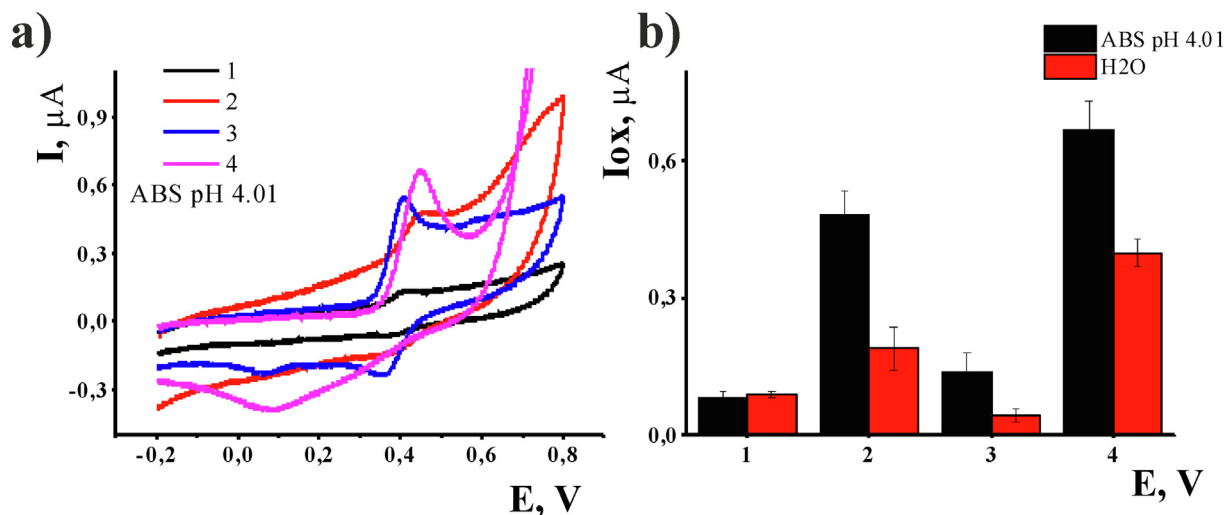


Fig. 8. Electronic absorption spectra for system ( $C_{\text{IPEC}} = 3 \times 10^{-6}$  M,  $C_{\text{guest}} = 3 \times 10^{-6}$  M): (a) IPEC + Q in water; (b) IPEC + Q in phosphate buffer solution (pH = 7.44); (c) IPEC + Q in acetate buffer solution (pH = 4.00); (d) IPEC + Q in phosphate buffer solution (pH = 8.15).



**Fig. 9.** (a) cyclic voltammograms and (b) quercetin oxidation peak currents on GCE in ABS pH 4.00 or H<sub>2</sub>O in presence of (1) 3  $\mu\text{M}$  and (3) 30  $\mu\text{M}$  quercetin or (2) 3  $\mu\text{M}$  and (4) 30  $\mu\text{M}$  IPEC + quercetin.

taining the absorption intensity of the interpolyelectrolyte in the absorption spectrum of the system, recorded a day after dilution. This indicates the destruction of the complex, the release and precipitation of quercetin over time.

The study of the acidic media effect on the IPEC + Q ternary system showed (Fig. 8c, S12) that in acetate buffer (pH = 4.00, pH = 5.00–5.50) quercetin was not released from the complex over time. Changing the pH medium to a more alkaline one (phosphate buffer, pH = 8.15) made it possible to establish that the quercetin band at 366 nm shifted to the red region of the spectrum with a simultaneous hypochromic effect during the first hour after diluting the ternary system with phosphate buffer. A new band at 330 nm appears at the same time in the absorption spectra (1 min to 1 h), which is probably due to the gradual oxidation of quercetin in solution upon release. The band at 366 nm almost completely disappears a day after the preparation of the solution.

Thus, the release of quercetin from the IPEC over time in neutral (pH = 7.44) and weakly alkaline (pH = 8.15) solutions was shown by electron absorption spectroscopy. It should be noted that the release of the flavonoid in a slightly alkaline solution was accompanied by the simultaneous oxidation of quercetin. On the other hand there is no release of quercetin from IPEC in an acidic (pH = 4.00) and weakly acidic (pH = 5.00–5.5) environment (Fig. S12). The fluorescence quenching of the IPEC in the presence of quercetin, shown earlier, can be used for ultrasensitive detection of metabolites. It will be possible to track the delivery of the flavonoid to the target organs for subsequent treatment by changing the fluorescence of the IPEC.

### 3.5. Voltammetric study of the antioxidant properties of quercetin in complex with IPEC

Antioxidant properties of quercetin can be assessed by its electrochemical activity in aqueous media. For this purpose, redox peaks have been recorded on bare glassy carbon electrode in solutions of free and encapsulated quercetin. In all the conditions, quercetin forms a pair of reversible peaks corresponded to the conversion of hydroquinone/quinone units in its structure (Fig. 9). On bare electrode, the peak currents are limited by low solubility of quercetin in water. Though encapsulation should prevent direct electron transfer, the use of the same concentration of lipid particles resulted in a high increase of the currents both in neutral and acidic media. As an example, the voltammograms recorded with 3 and 30  $\mu\text{M}$  solutions in acetic buffer are presented below together

with the comparison of appropriate peak currents. It should be noted that incapsulation does not affect the peak morphology and slightly increases the peak separation so that mechanism of quercetin oxidation remained the same. The possible explanation of the results includes better solubilization of the quercetin particles and their higher surface concentration against similar experiments with quercetin dissolved in appropriate buffer.

## 4. Conclusion

New interpolyelectrolyte non-toxic complexes based on the self-assembly of water-soluble oppositely charged pillar[5]arenes were obtained. The influence of the counterion nature on the stability of the systems and the size of the formed aggregates was shown. It was found that a larger size of the counterion in the carboxylate macrocycle led to the formation of larger particles. The interaction of pillar[5]arenes containing carboxyl and quaternary ammonium groups, as well as the interpolyelectrolyte formed by them, with quercetin was shown. It was established that the binding of quercetin by the IPEC occurred more efficiently ( $\text{pK}_a = 5.13$ ) than with individual macrocycles due to the greater stability of the associates formed by IPEC. The influence of the pH media on the ability of quercetin to be released from the IPEC was shown. It was found that in an acidic media (pH = 4.00), neither the quercetin release from IPEC nor its oxidation occurred. And there was a gradual release of the flavonoid over time in a neutral solution. The quercetin release with its simultaneous oxidation in solution was shown for a weakly alkaline solution, as indicated by the appearance of a new absorption band at 330 nm in the electronic absorption spectra. The results obtained, namely, the creation of an IPECs for encapsulation and dissolution of flavonoids (quercetin) in aqueous media, open up opportunities for obtaining multitarget drugs that can support the vital systems of patients with virus infection.

## Funding

The work was supported by the Russian Science Foundation (Grant No 18-73-10094, <https://rscf.ru/project/18-73-10094>).

## CRediT authorship contribution statement

**Anastasia Nazarova:** Investigation, Writing – original draft, Methodology, Visualization. **Luidmila Yakimova:** Investigation, Data curation, Supervision, Funding acquisition. **Oлга Mostovaya:**



Investigation. **Tatiana Kulikova:** Investigation, Software. **Olga Mikhailova:** Investigation. **Gennady Evtugyn:** Software. **Irina Ganeeva:** Investigation, Visualization. **Emil Bulatov:** Investigation, Data curation. **Ivan Stoikov:** Conceptualization, Writing – review & editing, Supervision.

### Data availability

The authors do not have permission to share data.

### Declaration of Competing Interest

The authors declare that they have no known competing financial interests or personal relationships that could have appeared to influence the work reported in this paper.

### Acknowledgements

The investigation of the compounds by fluorescence spectroscopy was carried out within the framework of the grants of the President of the Russian Federation for state support of young Russian scientists—candidates of sciences (MK-723.2021.1.3). Voltammetric study of the antioxidant properties of quercetin has been carried out by the Kazan Federal University Strategic Academic Leadership Program ('PRIORITY-2030').

### Appendix A. Supplementary material

Additional experimental details, Figure S1: Structure of pillar[5]arenes 1-3; Figures S2-S4: <sup>1</sup>H NMR spectra of the compounds **1-3**; Table S1: Sizes of aggregates and the corresponding polydispersity indices (PDI) of the IPEC; Figure S5: Electron absorption spectra of pillar[5]arene 1/quercetin and pillar[5]arene 3/quercetin in the presence of a 10-fold excess of guest; Table S2: Sizes of aggregates and the corresponding polydispersity indices (PDI) of the systems **1** + Quercetin, **3** + Quercetin and IPEC + Quercetin; Figure S6: <sup>1</sup>H NMR spectra 1, quercetin and their mixture; Figure S7: Fluorescence spectra of pillar[5]arene **1**/quercetin, pillar[5]arene **3**/quercetin and IPEC/quercetin in equimolar ratio in binary system (H<sub>2</sub>O + 5% EtOH); Figure S8: Fluorescence spectra of pillar[5]arene **3** with different concentrations of quercetin; Figures S9-S11: Bind-fit screenshots for the mixtures **3** + Quercetin, **1** + Quercetin and IPEC + Quercetin; Figure S12: Electronic absorption spectra for IPEC-quercetin system in acetate buffer at pH = 5.00 and pH = 5.50. Supplementary data to this article can be found online at <https://doi.org/10.1016/j.molliq.2022.120807>.

### References

- [1] X. Song, Y. Wang, L. Gao, Mechanism of antioxidant properties of quercetin and quercetin-DNA complex, *J. Mol. Model.* 26 (2020) 133, <https://doi.org/10.1007/s00894-020-04356-x>.
- [2] M. Azeem, M. Hanif, K. Mahmood, N. Ameer, F.R.S. Chughtai, U. Abid, An insight into anticancer, antioxidant, antimicrobial, antidiabetic and anti-inflammatory effects of quercetin: a review, *Polym. Bull.* (2022), <https://doi.org/10.1007/s00289-022-04091-8>.
- [3] B. Ozyel, G.L. Gall, P.W. Needs, P.A. Kroon, Anti-inflammatory effects of quercetin on high-glucose and pro-inflammatory cytokine challenged vascular endothelial cell metabolism, *Mol. Nutr. Food. Res.* 65 (2021) 2000777, <https://doi.org/10.1002/mnfr.202000777>.
- [4] B. Salehi, L. Machin, L. Monzote, J. Sharifi-Rad, S.M. Ezzat, M.A. Salem, R.M. Merghany, N.M. El Mahdy, C.S. Kiliç, O. Sytar, M. Sharifi-Rad, F. Sharopov, N. Martins, M. Martorell, W.C. Cho, Therapeutic potential of quercetin: new insights and perspectives for human health, *ACS Omega.* 5 (2020) 11849–11872, <https://doi.org/10.1021/acsomega.0c01818>.
- [5] K. Ferenczyova, B. Kalocayova, M. Bartekova, Potential implications of quercetin and its derivatives in cardioprotection, *Int. J. Mol. Sci.* 21 (2020) 1585, <https://doi.org/10.3390/ijms21051585>.
- [6] G. Derosa, P. Maffioli, A. D'Angelo, F. Di Pierro, A role for quercetin in coronavirus disease 2019 (COVID-19), *Phytother. Res.* 35 (2021) 1230–1236, <https://doi.org/10.1002/ptr.6887>.
- [7] M. Aucoin, K. Cooley, P.R. Saunders, V. Cardozo, D. Remy, H. Cramer, C.N. Abad, N. Hannan, The effect of quercetin on the prevention or treatment of COVID-19 and other respiratory tract infections in humans: a rapid review, *Adv. Integr. Med.* 7 (2020) 247–251, <https://doi.org/10.1016/j.aimed.2020.07.007>.
- [8] J.X. Yang, T.C. Maria, B. Zhou, F.L. Xiao, M. Wang, Y.J. Mao, Y. Li, Quercetin improves immune function in Arbor Acre broilers through activation of NF-κB signaling pathway, *Poultry Sci.* 99 (2020) 906–913, <https://doi.org/10.1016/j.psj.2019.12.021>.
- [9] P. Shen, W. Lin, X. Deng, X. Ba, L. Han, Z. Chen, K. Qin, Y. Huang, S. Tu, Potential implications of quercetin in autoimmune diseases, *Front. Immunol.* 12 (2021), <https://doi.org/10.3389/fimmu.2021.689044>.
- [10] C.H. Kim, J.-E. Kim, Y.-J. Song, Antiviral activities of quercetin and isoquercitrin against human herpesviruses, *Molecules.* 25 (2020) 2379, <https://doi.org/10.3390/molecules25102379>.
- [11] A. Rojas, J.A. Del Campo, S. Clement, M. Lemasson, M. Garcia-Valdecasas, A. Gil-Gomez, I. Ranchal, B. Bartosch, J.D. Bautista, A.R. Rosenberg, F. Negro, M. Romero-Gomez, Effect of quercetin on hepatitis C virus life cycle: from viral to host targets, *Sci. Rep.* 6 (2016) 31777, <https://doi.org/10.1038/srep31777>.
- [12] X. Chen, D.J. McClements, Y. Zhu, Y. Chen, L. Zou, W. Liu, C. Cheng, D. Fu, C. Liu, Enhancement of the solubility, stability and bioaccessibility of quercetin using protein-based excipient emulsions, *Food Res. Int.* 114 (2018) 30–37, <https://doi.org/10.1016/j.foodres.2018.07.062>.
- [13] A. Kellil, S. Grigorakis, S. Loupassaki, D.P. Makris, Empirical kinetic modelling and mechanisms of quercetin thermal degradation in aqueous model systems: effect of pH and addition of antioxidants, *Appl. Sci.* 11 (2021) 2579, <https://doi.org/10.3390/app11062579>.
- [14] S. Dall'Acqua, G. Miolo, G. Innocenti, S. Caffieri, The photodegradation of quercetin: relation to oxidation, *Molecules* 17 (2012) 8898–8907, <https://doi.org/10.3390/molecules17088898>.
- [15] Z. Zheng, W.-C. Geng, Z. Xu, D.-S. Guo, Macrocyclic amphiphiles for drug delivery, *Isr. J. Chem.* 59 (2019) 913–927, <https://doi.org/10.1002/ijch.201900032>.
- [16] A. Nazarova, D. Shurpik, P. Padnya, T. Mukhametzyanov, P. Gragg, I. Stoikov, Self-assembly of supramolecular architectures by the effect of amino acid residues of quaternary ammonium pillar[5]arenes, *Int. J. Mol. Sci.* 21 (2020) 7206, <https://doi.org/10.3390/ijms21197206>.
- [17] X. Fan, X. Guo, Development of calixarene-based drug nanocarriers, *J. Mol. Liq.* 1 (2021), <https://doi.org/10.1016/j.molliq.2020.115246>.
- [18] S. Lan, Y. Liu, K. Shi, D. Ma, Acetal-functionalized pillar[5]arene: a pH-responsive and versatile nanomaterial for the delivery of chemotherapeutic agents, *ACS Appl. Bio Mater.* 3 (2020) 2325–2333, <https://doi.org/10.1021/acsbm.0c00086>.
- [19] Y. Zhou, Q. Wang, L. Ma, J. Fan, Y. Han, C. Yan, Complexation of pillar[5]arene-based Schiff bases with methylene blue: formation of binary complexes with improved anticancer activity, *J. Mol. Struct.* 1257 (2022), <https://doi.org/10.1016/j.molstruc.2022.132588>.
- [20] N. Barooah, J. Mohanty, A.C. Bhasikuttan, Cucurbituril-based supramolecular assemblies: prospective on drug delivery, sensing, separation, and catalytic applications, *Langmuir.* 38 (2022) 6249–6264, <https://doi.org/10.1021/acs.langmuir.2c00556>.
- [21] A. Nazarova, A. Khannanov, A. Boldyrev, L. Yakimova, I. Stoikov, Self-assembling systems based on pillar[5]arenes and surfactants for encapsulation of diagnostic dye dapi, *Int. J. Mol. Sci.* 22 (2021) 6038, <https://doi.org/10.3390/ijms22116038>.
- [22] A.B. Mirgorodskaya, R.A. Kushnazarova, A.V. Nikitina, I.I. Semina, I.R. Nizameev, M.K. Kadirov, V.V. Khutoryanskiy, L.Y. Zakharova, O.G. Sinyashin, Polyelectrolyte nanocontainers: Controlled binding and release of indomethacin, *J. Mol. Liq.* 15 (2018) 982–989, <https://doi.org/10.1016/j.molliq.2018.10.115>.
- [23] A. M. Rumyantsev, N. E. Jackson, J. J. de Pablo, Polyelectrolyte complex coacervates: recent developments and new frontiers, *Annu. Rev. Condens. Ma. P.* 12 (2021) 155–176, <https://doi.org/10.1146/annurev-conmatphys-042020-113457>.
- [24] D. Wu, L. Zhu, Y. Li, X. Zhang, S. Xu, G. Yang, T. Delair, Chitosan-based colloidal polyelectrolyte complexes for drug delivery: a review, *Carbohydr. Polym.* 238 (2020), <https://doi.org/10.1016/j.carbpol.2020.116126>.
- [25] N. Khan, B. Brettmann, Intermolecular interactions in polyelectrolyte and surfactant complexes in solution, *Polymers.* 11 (2019) 51, <https://doi.org/10.3390/polym11010051>.
- [26] D.V. Pergushov, A.H.E. Müller, F.H. Schacher, Micellar interpolyelectrolyte complexes, *Chem. Soc. Rev.* 41 (2012) 6888–6901, <https://doi.org/10.1039/c2cs35135h>.
- [27] C. Li, X. Shu, J. Li, S. Chen, K. Han, M. Xu, X. Jia, Complexation of 1,4-bis(pyridinium)butanes by negatively charged carboxylatopillar[5]arene, *J. Org. Chem.* 76 (2011) 8458–8465, <https://doi.org/10.1021/jo201185e>.
- [28] D.N. Shurpik, L.S. Yakimova, I.K. Rizvanov, V.V. Plemenkov, I.I. Stoikov, Water-soluble pillar[5]arenes: synthesis and characterization of the inclusion complexes with *p*-toluenesulfonic acid, *Macroheterocycles.* 8 (2015) 128–134, <https://doi.org/10.6060/mhc140928>.
- [29] Y. Chen, S. Sun, D. Lu, Y. Shi, Y. Yao, Water-soluble supramolecular polymers constructed by macrocycle-based host-guest interactions, *Chinese Chem. Lett.* 30 (2019) 37–43, <https://doi.org/10.1016/j.ccllet.2018.10.022>.

- [30] L. Shao, Y. Pan, B. Hua, S. Xu, G. Yu, M. Wang, B. Liu, F. Huang, Constructing adaptive photosensitizers via supramolecular modification based on pillararene host-guest interactions, *Angew. Chem. Int. Ed.* 59 (2020) 11779–11783, <https://doi.org/10.1002/anie.202000338>.
- [31] X. Shu, K. Xu, D. Hou, C. Li, Molecular recognition of water-soluble pillar[n]arenes towards biomolecules and drugs, *Isr. J. Chem.* 58 (2018) 1230–1240, <https://doi.org/10.1002/ijch.201800115>.
- [32] D. Zhang, J. Cheng, L. Wei, W. Song, L. Wang, H. Tang, D. Cao, Host-guest complexation of monoanionic and dianionic guests with a polycationic pillararene host: same two-step mechanism but striking difference in rate upon inclusion, *J. Phys. Chem. Lett.* 11 (2020) 2021–2026, <https://doi.org/10.1021/acs.jpcllett.0c00277>.
- [33] Bindfit v0.5. Available online: <http://supramolecular.org/bindfit> (Accessed on 25 May 2022).
- [34] E.A. Andreyko, P.L. Padnya, I.I. Stoikov, Amphiphilic p-tert-butylthiacalix[4]arenes containing quaternary ammonium groups: from small molecules toward water-soluble nanoscale associates, *J. Phys. Org. Chem.* 28 (2015) 527–535, <https://doi.org/10.1002/poc.3433>.
- [35] A.A. Nazarova, L.I. Makhmutova, I.I. Stoikov, Synthesis of pillar[5]arenes with a PH-containing fragment, *Russ. J. Gen. Chem.* 87 (2017) 1941–1945, <https://doi.org/10.1134/S1070363217090080>.
- [36] A.A. Nazarova, L.S. Yakimova, P.L. Padnya, V.G. Evtugyn, Y.N. Osin, P.J. Cragg, I.I. Stoikov, Monosubstituted pillar[5]arene functionalized with (amino) phosphonate fragments are “smart” building blocks for constructing nanosized structures with some s- and p-metal cations in the organic phase, *New J. Chem.* 43 (2019) 14450–14458, <https://doi.org/10.1039/c9nj03539g>.
- [37] R.R. Zairov, R.N. Nagimov, S.N. Sudakova, D.V. Lapaev, V.V. Syakaev, G.S. Gimazetdinova, A.D. Voloshina, M. Shykula, I.R. Nizameev, A.I. Samigullina, A. T. Gubaidullin, S.N. Podyachev, A.R. Mustafina, Polystyrenesulfonate-coated nanoparticles with low cytotoxicity for determination of copper(II) via the luminescence of Tb(III) complexes with new calix[4]arene derivatives, *Microchim. Acta.* 185 (2018) 386, <https://doi.org/10.1007/s00604-018-2923-2>.
- [38] B. Bolshchikov, S. Volkov, D. Sokolova, A. Gorbunov, A. Serebryannikova, I. Glorizov, D. Cheshkov, S. Bezzubov, W.S. Chung, V. Kovalev, I. Vatsouro, Constructing bridged multifunctional calixarenes by intramolecular indole coupling, *Org. Chem. Front.* 6 (2019) 3327–3341, <https://doi.org/10.1039/C9QO00859D>.
- [39] J.F. Chen, Q. Lin, H. Yao, Y.M. Zhang, T.B. Wei, Pillar[5]arene-based multifunctional supramolecular hydrogel: multistimuli responsiveness, self-healing, fluorescence sensing, and conductivity, *Mater. Chem. Front.* 2 (2018) 999–1003, <https://doi.org/10.1039/C8QM00065D>.
- [40] C. Hu, Z. Li, Z. Hu, Q. Li, Y. Fu, Z. Chen, Synthesis of multifunctional crown ether covalent organic nanospheres as stationary phase for capillary electrochromatography, *J. Chromat. A.* 1677 (2022), <https://doi.org/10.1016/j.chroma.2022.46332>.
- [41] X. Hu, G. Xu, H. Zhang, M. Li, Y. Tu, X. Xie, Y. Zhu, L. Jiang, X. Zhu, X. Ji, Y. Li, A. Li, Multifunctional  $\beta$ -cyclodextrin polymer for simultaneous removal of natural organic matter and organic micropollutants and detrimental microorganisms from water, *ACS Appl. Mater. Interfaces.* 12 (2020) 12165–12175, <https://doi.org/10.1021/acsami.0c00597>.
- [42] J. Peng, Y. Liu, M. Zhang, F. Liu, L. Ma, C.Y. Yu, H. Wei, One-pot fabrication of dual-redox sensitive, stabilized supramolecular nanocontainers for potential programmable drug release using a multifunctional cyclodextrin unit, *J. Control. Release.* 334 (2021) 290–302, <https://doi.org/10.1016/j.jconrel.2021.04.027>.
- [43] C. Liu, P. Wang, X. Liu, X. Yi, Z. Zhou, D. Liu, Multifunctional  $\beta$ -cyclodextrin MOF-derived porous carbon as efficient herbicides adsorbent and potassium fertilizer, *ACS Sustain. Chem. Eng.* 7 (2019) 14479–14489, <https://doi.org/10.1021/acsuschemeng.9b01911>.
- [44] S. Datz, B. Illes, D. Gößl, C. Schirnding, H. Engelke, T. Bein, Biocompatible crosslinked  $\beta$ -cyclodextrin nanoparticles as multifunctional carriers for cellular delivery, *Nanoscale.* 10 (2018) 16284–16292, <https://doi.org/10.1039/C8NR02462F>.
- [45] D. Sbravati, A. Bonardi, S. Bua, A. Angeli, M. Ferraroni, A. Nocentini, A. Casnati, P. Gratteri, F. Sansone, C.T. Supuran, Calixarenes incorporating sulfonamide moieties: versatile ligands for carbonic anhydrases inhibition, *Chem. – Eur. J.* 28 (2021) 202103527, <https://doi.org/10.1002/chem.202103527>.
- [46] S.N. Podyachev, R.R. Zairov, A.R. Mustafina, 1,3-Diketone calix[4]arene derivatives—a new type of versatile ligands for metal complexes and nanoparticles, *Molecules.* 26 (2021) 1214, <https://doi.org/10.3390/molecules26051214>.
- [47] L. Yakimova, P. Padnya, D. Tereshina, A. Kunafina, A. Nugmanova, Y. Osin, V. Evtugyn, I. Stoikov, Interpolyelectrolyte mixed nanoparticles from anionic and cationic thiacalix[4]arenes for selective recognition of model biopolymers, *J. Mol. Liq.* 279 (2019) 9–17, <https://doi.org/10.1016/j.molliq.2019.01.099>.
- [48] D.N. Shurpik, P.L. Padnya, I.I. Stoikov, P.J. Cragg, Antimicrobial activity of calixarenes and related macrocycles, *Molecules.* 25 (2020) 5145, <https://doi.org/10.3390/molecules25215145>.
- [49] H. Zhang, Z. Liu, Y. Zhao, Pillararene-based self-assembled amphiphiles, *Chem. Soc. Rev.* 47 (2018) 5491–5528, <https://doi.org/10.1039/C8CS00037A>.
- [50] A.D. Kulkarni, Y.H. Vanjari, K.H. Sancheti, H.M. Patel, V.S. Belgamwar, S.J. Surana, C.V. Pardeshi, Polyelectrolyte complexes: mechanisms, critical experimental aspects, and applications, *Artif. Cells Nanomed Biotechnol.* 44 (2016) 1615–1625, <https://doi.org/10.3109/21691401.2015.1129624>.
- [51] T. Ogoshi, S. Kanai, S.h. Fujinami, T. Yamagishi, Y. Nakamoto, para-bridged symmetrical pillar[5]arenes: their Lewis acid catalyzed synthesis and host-guest property, *J. Am. Chem. Soc.* 130 (2008) 5022–5023, <https://doi.org/10.1021/ja711260m>.
- [52] R.N. Dsouza, U. Pischel, W.M. Nau, Fluorescent dyes and their supramolecular host/guest complexes with macrocycles in aqueous solution, *Chem. Rev.* 111 (2011) 7941–7980, <https://doi.org/10.1021/cr200213s>.
- [53] S. Shah, L. Leon, Structural dynamics, phase behavior, and applications of polyelectrolyte complex micelles, *Curr. Opin. Colloid In.* 53 (2021), <https://doi.org/10.1016/j.cocis.2021.101424>.
- [54] A.E. Marras, J.M. Ting, K.C. Stevens, M.V. Tirell, Advances in the structural design of polyelectrolyte complex micelles, *J. Phys. Chem.* 125 (2021) 7076–7089, <https://doi.org/10.1021/acs.jpcc.1c01258>.
- [55] S. Yi, J. Zheng, P. Lv, D. Zhang, X. Zheng, Y. Zhang, R. Liao, Controlled drug release from cyclodextrin-gated mesoporous silica nanoparticles based on switchable host-guest interactions, *Bioconjugate Chem.* 29 (2018) 2884–2891, <https://doi.org/10.1021/acs.bioconjchem.8b00416>.
- [56] J. Zhang, Y. Lin, Z. Lin, Q. Wei, J. Qian, R. Ruan, X. Jiang, L. Hou, J. Song, J. Ding, H. Yang, Stimuli-responsive nanoparticles for controlled drug delivery in synergistic cancer immunotherapy, *Adv. Sci.* 9 (2021) 2103444, <https://doi.org/10.1002/adv.202103444>.
- [57] B. Naseem, S.W.H. Shah, A. Hasan, S.S. Shah, Interaction of flavonoids, the naturally occurring antioxidants with different media: a UV-visible spectroscopic study, *Spectrochim. Acta A: Mol. Biomol. Spectrosc.* 75 (2010) 1341–1346, <https://doi.org/10.1016/j.saa.2009.12.083>.